Phosphine-Free Manganese Catalyst Enables Selective Transfer Hydrogenation of Nitriles to Primary and Secondary Amines Using Ammonia–Borane

Koushik Sarkar,[§] Kuhali Das,[§] Abhishek Kundu, Debashis Adhikari,* and Biplab Maji*

Read Online

ACCESS | Metrics & More | Article Recommendations | SI Supporting Information

ABSTRACT: Herein we report the synthesis of primary and secondary amines by nitrile hydrogenation, employing a borrowing hydrogenation strategy. A class of phosphine-free manganese(I) complexes bearing sulfur side arms catalyzed the reaction under mild reaction conditions, where ammonia−borane is used as the source of hydrogen. The synthetic protocol is chemodivergent, as the final product is either primary or secondary amine, which can be controlled by changing the catalyst structure and the polarity of the reaction medium. The significant advantage of this method is that the protocol operates without externally added base or other additives as well as obviates the use of high-pressure dihydrogen gas required for other nitrile hydrogenation reactions. Utilizing this method, a wide variety of primary and symmetric and asymmetric secondary amines were synthesized in high yields. A mechanistic study involving kinetic experiments and high-level DFT computations revealed that both outer-sphere dehydrogenation and inner-sphere hydrogenation were predominantly operative in the catalytic cycle.

KEYWORDS: *amine, hemilability, transfer hydrogenation, manganese, kinetics, DFT*
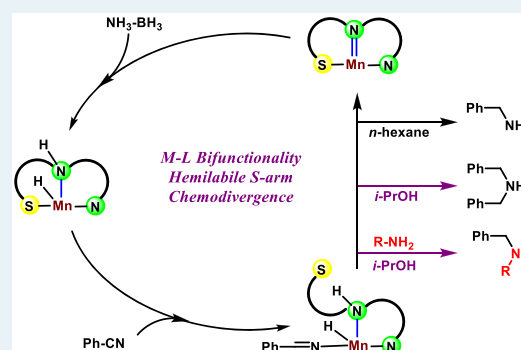
The demand for a greener and more sustainable chemical synthesis inarguably requires reengineering the known catalytic pathways so that the use of critical elements can be minimized. Achieving this goal calls for using earth-abundant transition metals in homogeneous catalysis as a surrogate to their precious metal analogues.[1] Less toxicity and the promise of displaying new catalytic activity additionally make their use intriguing.[2] In this regard, the molecularly defined complexes of the third most abundant transition metal manganese have gathered tremendous attention in waste-free redox transformations.[3] Following the pioneering work on dehydrogenative imine synthesis by Milstein,[4] and the hydrogenation reaction by Beller,[5] homogeneous manganese(I) complexes have been utilized in many (de)hydrogenation reactions.[3] To augment bond activation in elementary steps, such as in hydrogen activation and hydrogen transfer, phosphine-based multidentate ligands were utilized in many of those nonprecious metal catalysis.[6] However, limited availability and difficulties in their preparation under ambient conditions make those phosphine-based ligands expensive, often by many fold, so that the cost benefits of nonprecious metals are forfeited. Accordingly, to leverage abundant 3d metals as a sustainable solution, using economic and readily available ligands is crucial, and their synthesis and use are highly demanded. Toward this end, we[7] and others[8] have recently advocated for the phosphine-free manganese catalysis for

acceptorless dehydrogenative coupling and the borrowing hydrogenation reaction. Recently, apart from the metal−ligand bifunctional co-operativity, we have successfully demonstrated the hemilability of a soft thiophene donor side arm as a key design principle for the **Mn1** (Scheme 1c)-catalyzed synthesis of (1+n)-membered cycloalkanes[9] and β-branched carbonyl compounds.[10] In the quest for efficient manganese catalysts in nitrile hydrogenation, we develop a set of phosphine ligand-free catalysts (**Mn1** and **Mn2**, Scheme 1c) bearing a soft sulfur donor side arm in the ligand backbone.[11] Encouragingly, our developed synthetic protocol is chemodivergent in nature. Both primary and secondary amines were synthesized selectively using ammonia−borane (H₃N·BH₃; AB) as the hydrogen source (Scheme 1).

The hydrogenation of nitriles has been recognized as an appealing route to synthesizing high-value amine building blocks.[12] However, controlling the selectivity of such processes remains challenging owing to the formation of primary,
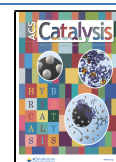
Scheme 1. Homogeneous Hydrogenation of Nitriles to Divergent Amines

free base metal complexes for the hydrogenation of nitriles have not been developed thus far.

■ RESULTS AND DISCUSSION

Reaction Optimization. We commenced our investigation using benzonitrile **1a** as the model substrate. To our delight, manganese catalyst **Mn1** at 3 mol% loadings displayed excellent catalytic activity for the selective hydrogenation of **1a** in hexane solution at 60 °C (Table 1, entry 1). It delivered

Table 1. Key Optimization for Selective Synthesis of Primary and Secondary Amines[a]

entry	[Mn]	solvent	conversion of 1a (%)[b]	yield[b] (%) 2a	yield[b] (%) 3a
1	Mn1	n-hexane	>99	90	n.d.
2	Mn2	n-hexane	>99	92	n.d.
3	Mn3	n-hexane	80	30	n.d.
4	Mn4	n-hexane	85	26	n.d.
5	Mn2	toluene	>99	90	n.d.
6	Mn2	THF	>99	90	n.d.
7[d]	Mn2	2-propanol	80	n.d.	49 (42)[c]
8[d]	Mn1	2-propanol	98	n.d.	91 (85)[c]
9[d]	Mn1	ethanol	78	n.d.	74
10[d]	Mn3	2-propanol	93	n.d.	61
11[d]	Mn4	2-propanol	88	n.d.	47

Reaction conditions: **1a** (0.1 mmol), [Mn] (3 mol %), H₃N·BH₃ (0.3 mmol), solvent (1 M), Ar, 60 °C, 6 h. [b]Conversion, and yields were determined by gas chromatography using mesitylene as an internal standard. [c]Isolated yield. [d]Reaction time 12 h. n.d. = not detected.

secondary, and tertiary amine product mixtures (Scheme 1a). Early studies on homogeneous nitrile hydrogenation utilized catalysts comprising second- and third-row-transition metals, where various reaction parameters, including ligand structure, hydrogen pressure, temperature, and additives, were adjusted to tune the selectivity (Scheme 1b).[13] Very recently, the groups of Beller,[14] Milstein,[15] Fout,[16] Guan,[17] Kirchner,[18] Garcia,[19] and Huang[20] have introduced molecularly defined non-noble Fe, Mn, and Co catalysts for the hydrogenation of nitriles to primary amines using up to 60 bar of hydrogen gas pressure and up to 120 °C temperature. In comparison to the direct hydrogenation by H₂, the transfer hydrogenation, which operates under ambient conditions, bypassing the need for flammable hydrogen gas under higher pressure conditions, is valued as an alternative strategy.[21]

Initially, such reactions utilized ruthenium-based homogeneous catalysts with alcohols as the hydrogen source.[21a,b] Recently, AB, which has primarily been studied as an appropriate solid hydrogen storage material due to its high hydrogen content (19.6% by weight), low toxicity, and high stability, has found applications as an ideal dihydrogen source for transfer hydrogenation reactions.[21c−h,22] In this regard, only two base−metal-catalyzed transfer hydrogenation of nitriles have been recently reported using homogeneous phosphine-derived cobalt catalysts.[21c,e] The reported manganese(I) nitrile hydrogenation catalysts using molecular hydrogen[5,18,19] and alcohol[21f] as the hydrogen source were only selective for the synthesis of primary amines and offered limited scope owing to the use of multidentate alkylphosphine-derived ligands, high temperature (and high hydrogen pressure), and base as an additive. Herein we disclose manganese-catalyzed chemo-divergent hydrogenation of nitriles to forge both primary and secondary amines under mild and additive-free conditions (Scheme 1c). The crucial role of the soft sulfur donor in the side arm has been delineated by comparing the activities of **Mn1** and **Mn2** with their oxygen analogues **Mn3** and **Mn4** and through a detailed kinetic and high-level computational mechanistic study. To the best of our knowledge, phosphine-

the desired primary amine **2a** in 90% yield without any trace of the undesired homodimer **3a**. Complex **Mn2** with a thiomethoxy side arm showed better catalytic activity, as the yield of **2a** was improved to 92% without any loss of selectivity (entry 2). However, the structurally similar manganese complexes **Mn3** and **Mn4**, without the soft sulfur donor atom at the side arm, exhibited poorer catalytic activity as reflected through both the lower conversion of **1a** and significantly diminished yield of **2a** (entries 3 and 4). This reduction of efficiency highlights the profound role of the sulfur-containing side arm in the catalytic activity (vide infra).

Interestingly, the reaction medium was found to influence the selectivity between primary and secondary amines significantly. While aprotic solvents such as toluene and THF delivered the primary amine in high yields (entries 5 and 6), the protic solvents (entries 7−9) switched the selectivity to secondary amines. For example, dibenzylamine **3a** was obtained in 49% yield after 12 h when 2-propanol was used as a solvent, keeping other reaction conditions identical (entry 7). Pleasingly, the yield of **3a** was improved to 91% when **Mn1**

was used as a catalyst (entry 8). Thus, the protocol allowed catalyst/solvent-controlled chemodivergent access to both primary and secondary amines under milder reaction conditions. The beneficial effect of the soft donor side arm was also observed in the synthesis of secondary amines, as a lower yield of 3a was observed when Mn3 and Mn4 were used as the catalysts (entries 10 and 11). Further details of the reaction optimization, including the variation of temperature, stoichiometry, solvent, and concentration, are tabulated in Tables S1−S7.

Scope of the Reaction. With the set of optimized reaction conditions in hand, the reaction's feasibility to various nitriles was explored. Table 2 summarizes the Mn2-catalyzed hydrogenation of nitriles 1 to primary amines 2 in hexane. A broad range of substrates containing electronically biased functional groups was efficiently converted to the corresponding primary amines 2, isolated as the ammonium salt 2′ in up to 98% yield. Aromatic nitriles bearing electron-donating groups at the ortho-, meta-, and para-position of the aromatic ring resulted in the complete conversion of nitriles 1b−f, and the corresponding ammonium salts 2′b−f were isolated in 85−98% yields. Substrates bearing different halogens such as chloro (1g), bromo (1h), fluoro (1i−k), and iodo (1l) groups at different positions of the aromatic ring were also well-tolerated, giving the corresponding ammonium salts 2′g−l in up to 91% isolated yield with the complete retention of halogen groups. For the substrate having a lactone-fused benzene ring 1m, the lactone survived under the reaction conditions, providing ammonium salt 2′m in 50% yield. However, for 4-acetylbenzonitrile 1n substrate, the keto group's reduction took place, and product 2n was isolated in 76% yield.

The reaction also tolerates aliphatic nitriles. Under the same conditions, phenyl acetonitrile 1o and 2-phenyl propionitrile 1p were efficiently converted to the corresponding primary amines in high yields. Several phenylacetonitrile derivatives containing methyl (1q), methoxy (1r−t), and halogen (1u−x) substituents at different positions of the aryl ring afforded the desired products 2′q−x in good to excellent yields. Aliphatic dinitrile 2,2′-(1,4-phenylene)diacetonitrile 1y also gave a satisfactory yield of the diamine product. Moreover, 1-naphthylacetonitrile 1z was also converted to the corresponding ammonium salt in 85% yield. Gratifyingly, the hydrogenation of adiponitrile 1za also proceeded smoothly under the optimized conditions in Table 1, and hexamethylenediamine was isolated in 95% yield as its hydrochloride salt.

The optimized reaction conditions in entry 8 of Table 1 were then exploited to synthesize various symmetrical secondary amines 3, and the results are summarized in Table 3. The reaction tolerates various electron-rich aromatic nitriles, yielding the corresponding secondary amines 3b−d in 85−94% yields with high selectivity. Likewise, electron-deficient nitriles, including fluoro, chloro, and bromo functionalities, were also well-tolerated in this reaction methodology, and the corresponding amines 3e−h were isolated in moderate to high (52−91%) yields. It is worth noticing that the halogen functional groups were retained in the products. Aromatic nitriles bearing an ester functionality were also converted to the symmetric secondary amine 3i in 65% yield with retention of the ester group.

Encouraged by the efficiency of the developed methodology to yield symmetrical secondary amines 3, we were further prompted to explore the possibility of synthesizing unsymmetrical secondary amines 4 by adding an external amine 6

Table 2. Manganese-Catalyzed Synthesis of Primary Amines[a]
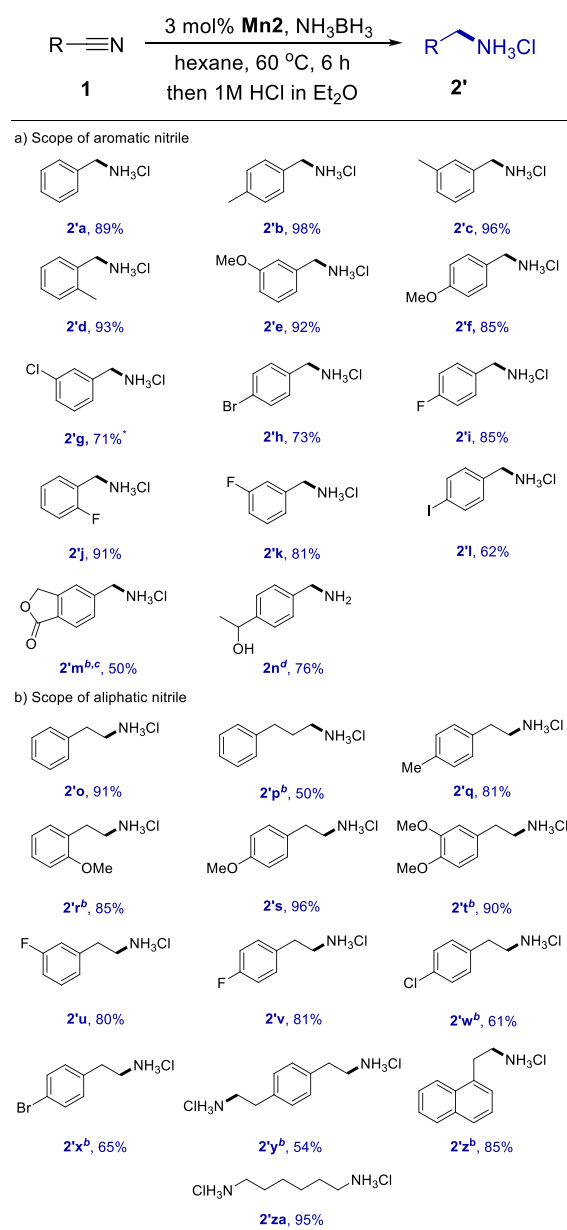
[a]Reaction conditions: 1 (0.25 mmol), Mn2 (3 mol %), H₃N·BH₃ (0.75 mmol), hexane (1 M), 60 °C, 6 h. Isolated yields of ammonium salt. [b]Reaction time 12 h. [c]59% conversion via gas chromatography using decane as an internal standard. [d] Free amine was isolated.

(Table 4). Benzonitrile 1a and 4-methoxybenzylamine 6a were chosen as model substrates to prepare the unsymmetrical amine. Pleasingly, manganese complex Mn2 was found to catalyze this reaction at 80 °C in 2-propanol, and the desired unsymmetrical amine 4a was isolated in 66% yield (see Table S8 for details). The reaction was general, as a host of primary amines with different substituents offered the desired products in synthetically acceptable yields. For example, electron-deficient 2-chlorobenzylamine 6b, pyridine-containing heterocyclic amine 6c, and aliphatic amines such as cyclohexylamine 6d and n-butylamine 6e were reacted with 1b, and the desired secondary amines 4b−e were isolated in moderate yields. The reaction could also be performed with different nitriles,

Table 3. Manganese-Catalyzed Synthesis of Symmetrical Secondary Amines 3[a]

3a, 85%   3b, 85%   3c, 87%

3d, 94%   3e, 72%   3f, 72%

3g, 52%   3h, 91%   3i, 65%
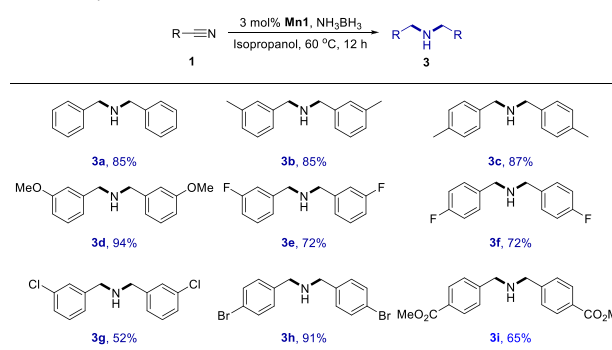
[a]Reaction conditions: **1** (0.25 mmol), **Mn1** (3 mol %), H$_3$N·BH$_3$ (0.75 mmol), 2-propanol (1 M), 60 °C, 12 h. Isolated yields.

Table 4. Manganese-Catalyzed Synthesis of Unsymmetrical Secondary Amines 4[a]

4a, 66%   4b, 52%   4c, 60%

4d, 55%   4e, 54%   4f, 52%

4g, 50%   4h, 65%   4i, 63%
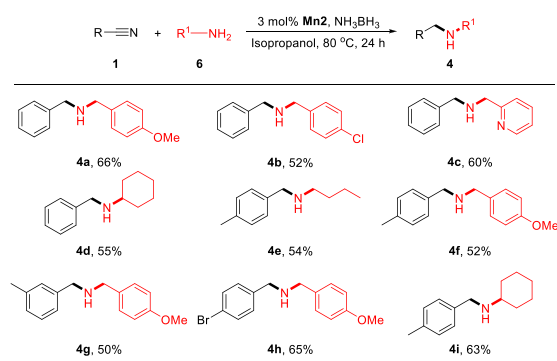
[a]Reaction conditions: **1** (0.25 mmol), **6** (0.375 mmol), **Mn2** (3 mol %), H$_3$N·BH$_3$ (0.75 mmol), 2-propanol (0.25 M), 80 °C, 24 h. Isolated yields.

delivering the desired products **4f–i** in 50−65% yields. However, aniline could not be used as a coupling partner under these conditions. Notably, the formation of symmetrical

secondary amine **3** was not detected in any of the reactions mentioned above.

Mechanistic Studies. Several experimental and high-level computational studies were then undertaken to probe the reaction mechanism. Kinetic analysis of the **Mn2**-catalyzed transfer hydrogenation of benzonitrile **1a** to benzylamine **2a** was performed in THF solution (Figure 1). We have observed an induction time, which might stem from the necessity of precatalyst activation. The points representing the induction time were discarded to obtain a linear fit during the kinetic analysis. For the reaction performed at [**1a**] = 0.25 M, [AB] = 0.75 M, the initial rate for the formation of **2a** was found to increase linearly with the increasing concentration of **Mn2** (0− 0.025 M). When the reaction was performed with a varying initial concentration of AB (0−1.0 M), the reaction was found to be first-order with [AB]. On the other hand, the initial rate for the formation of **2a** was independent of [**1a**]. Thus, an empirical rate law can be derived, as shown in eq 1. The above results suggest that nitrile hydrogenation may not be involved in the rate-limiting step. To the best of our knowledge, there is only one example of kinetic experiments for the homogeneous molybdenum-catalyzed transfer hydrogenation of nitrile involving AB as the hydrogen source, where similar rate dependence was observed.[21d]

When the kinetic experiments for the formation of **2a** were performed in toluene, we also observed first-order and zero-order kinetics with respect to **Mn2** and **1a**, respectively (Figure 1, eq 2). Surprisingly, the initial rates were found to be independent of the concentration of AB as well. This can be attributed to the poor solubility of AB in toluene, where the rate is governed by the saturation of AB in the reaction medium. Guan et al. have observed zeroth-order dependency of AB during iron bis(phosphinite) pincer complex-catalyzed dehydrogenation of AB, where rapid interaction of AB with the iron catalyst prior to the rate-determining step is suggested.[23]

$$\text{rate} = k[\mathbf{Mn2}]^1[\mathbf{1a}]^0[\text{AB}]^1 \quad (1)$$

$$\text{rate} = k[\mathbf{Mn2}]^1[\mathbf{1a}]^0[\text{AB}]^0 \quad (2)$$

High-level DFT computational studies were undertaken to delineate further details of the AB dehydrogenation and nitrile
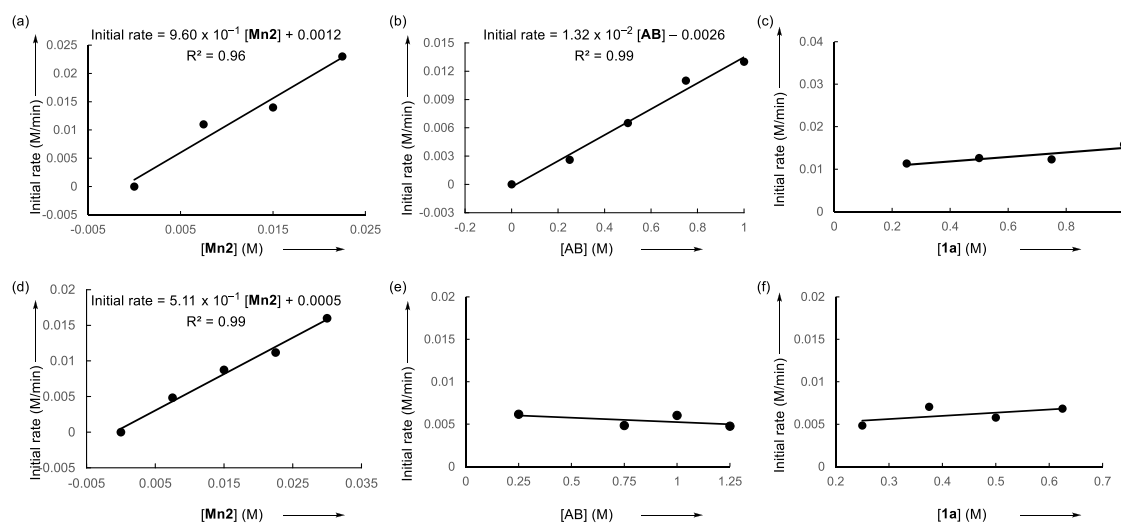
Figure 1. Kinetic analysis for the **Mn2**-catalyzed transfer hydrogenation of **1a** with AB: Plots show the rate of formation of **2a** vs concentration of (a) **Mn2**, (b) AB, and (c) **1a** in THF, and the rate of formation of **2a** vs concentration of (d) **Mn2**, (e) AB, and (f) **1a** in toluene.
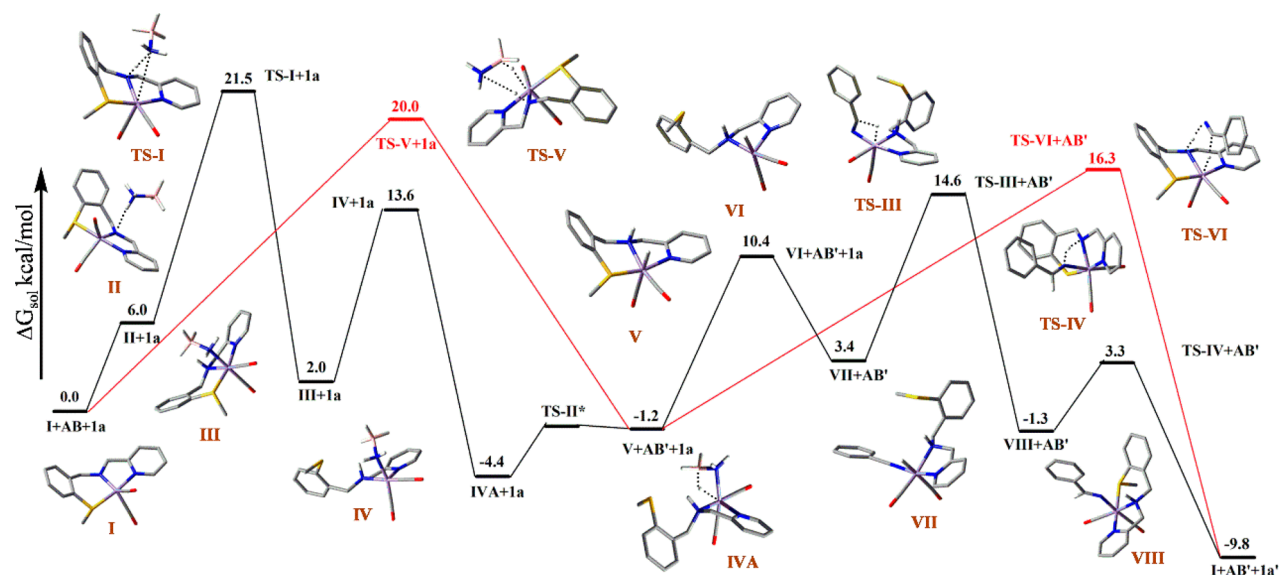
Figure 2. Potential energy surface at B3LYP level of theory for ammonia–borane dehydrogenation and subsequent hydrogenation of the nitrile **1a**, following borrowing hydrogen. The red trace describes the outer-sphere pathway for these two consecutive steps while the black trace designates the inner-sphere trajectory. **TS-II*** was not located but is shown in the diagram for illustration only.

hydrogenation reaction cascade. The best-performing **Mn2** has been chosen as the model catalyst in this study. The computations were performed at B3LYP level of theory with lanl2dz(Mn)+6-31G*(C, H, N, O, S) basis set (see details in Supporting Information (SI)). Treatment of **Mn2** with AB results in a pentacoordinate Mn(I) resting state upon loss of CO and Br ligands. The resting state (**I**) is prepared from the precatalyst by a supposed dehydrohalogenation promoted by a mild base. It is assumed that the small amount of NH_3 generated from the dissociation of AB promotes dehydrohalogenation. Indeed, the generation of the free base NMe_2H due to the dissociation of B−N bond from $H_3B \cdot NMe_2H$ has been documented previously.[24] As supporting evidence, we gathered some experimental proof to evaluate the catalytic resting state, where two new CO stretching frequencies (1996 and 1872 cm^{-1}) were observed upon treatment of **Mn2** with AB at 60 °C for 2 h. This mode of preactivation of the catalyst is advantageous because the substrate itself can convert the precatalyst to the amido form without any externally added base.

As optimized computationally, the resting state is a Y-shaped TBP geometry across manganese where the CO−Mn−CO bond angle is 92.42°. As anticipated, this geometry remains on the singlet spin surface because all six d-electrons of Mn(I) are paired under this geometrical influence. Similar Y-shaped geometry for catalyst **Mn1** has also been documented previously in our recent report.[9] It is noteworthy that the thiomethoxy arm is bound to electron-rich Mn(I), leading to a distorted trigonal bipyramidal geometry. This Y-type geometry is a consequence of strong π-donor amido in the ligand backbone, trans to the CO−Mn−CO angle, and the π-donor nature is evident further from the short Mn−N bond length (1.87 Å). The Mn−S bond length is 2.36 Å, indicating reasonably weak coordination. Our exploration to get a triplet geometry for **I** resulted in a square planar system with an unbound thiomethoxy arm, and it is much higher in energy than that of the singlet ground-state structure.

When the reactants are infinitely apart, the combined energy of **I**, AB, and **1a** has been considered as the reference state.

There are two choices to achieve AB dehydrogenation: outer-sphere pathway (red trace in the PES, Figures 2 and 3), where
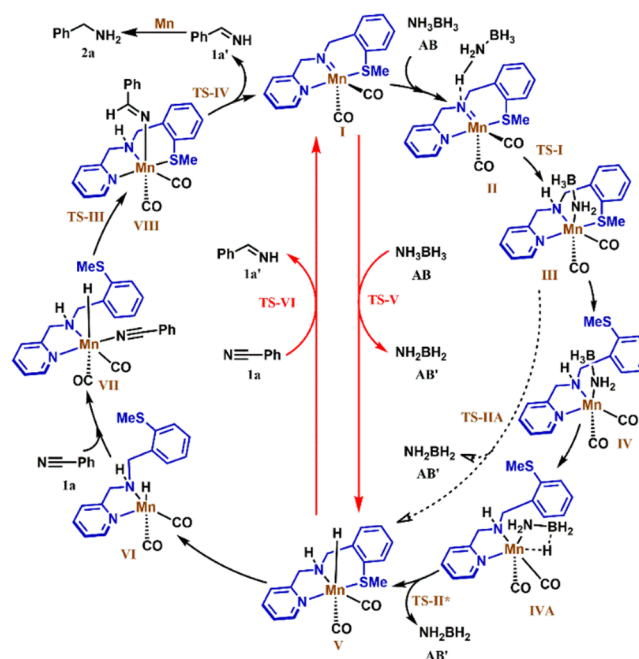
Figure 3. Catalytic cycle for AB dehydrogenation and nitrile hydrogenation.

a concerted hydrogen addition happens across the manganese−amido bond, or an inner-sphere pathway (a black trace in Figures 2 and 3), where the binding of AB to the metal center is required prior to β-hydride elimination.

To initiate the dehydrogenation step via the inner-sphere pathway, AB binds to **I** via weak intermolecular H-bonding, generating preparatory intermediate **II** for the proton transfer process. This weak binding costs 6.0 kcal/mol in energy from the reference state. In a recent report, such a weak interaction has been ascribed to initiation of dehydrogenation of AB.[25]

The proton transfer from the weakly bound AB to amido-N is a high energy process. The respective transition state (**TS-I**) for proton transfer exhibits an energy barrier of 21.5 kcal mol^{-1}. After proton transfer, the deprotonated AB binds to Mn(I) in an η^1 fashion, giving intermediate **III** where the amido linkage has been fully converted to the amine. This assertion is fully reflected in the Mn–N bond length (2.10 Å) in optimized intermediate **III**, which has been changed from 1.87 Å in **I**.

To facilitate the β-hydride elimination, the thiomethoxy arm of the ligand decoordinates and creates room across the manganese center, generating intermediate **IV**, where AB is bound to manganese through the nitrogen end. Intermediate **IV** slightly rearranges and stabilizes it further by creating a β-agostic interaction with the manganese, leaving intermediate **IVA**. Notably, this is the preparatory stage of β-hydride elimination, where a clear agostic interaction of B–H (B–H bond, closer to Mn, is elongated to 1.32 Å, while the Mn–H distance 1.71 Å) is noticed. It seems that an actual kite-like transition state to initiate β-hydride elimination lies on a very shallow potential energy surface and eluded optimization, despite multiple trials. However, due to the flat nature of the potential energy surface during this step, the barrier for such a TS is not high and will not dictate the significant energy demand of the reaction.[26] So, the inner-sphere pathway poses a barrier of 21.5 kcal mol^{-1}.

Interestingly, we were able to optimize the TS for β-hydride elimination (**TS-IIA**, not shown in PES) when the thiomethoxy arm is bound to manganese (a seven-coordinate species), and it poses a large barrier of 27.9 kcal mol^{-1} so that this pathway can safely be discarded. After β-hydride elimination, the thiomethoxy arm rebounds to engender intermediate **V**, which is a six-coordinate Mn-hydride. The alternative, outer-sphere pathway traverses through **TS-V** with a barrier of 20.0 kcal mol^{-1}. The TS is concerted in nature but highly asynchronous in transferring two hydrogens to nitrogen and manganese, respectively. From the energy values for dehydrogenation of AB, we conclude that the outer-sphere pathway is slightly favored over the inner-sphere one, although the energy difference is not large.

This observation is also supported by the experimental determination of the kinetic isotope effect when AB was appropriately labeled with deuterium (Figure 4). The overall kinetic isotope effect KIE ($k_{NH\cdot BH}/k_{ND\cdot BD}$ = 3.2) with the doubly labeled substrate is the product of KIE$_1$ ($k_{NH\cdot BH}/k_{NH\cdot BD}$ = 2.4) and KIE$_2$ ($k_{NH\cdot BH}/k_{ND\cdot BH}$ = 1.5), while KIE$_1$ reflects the
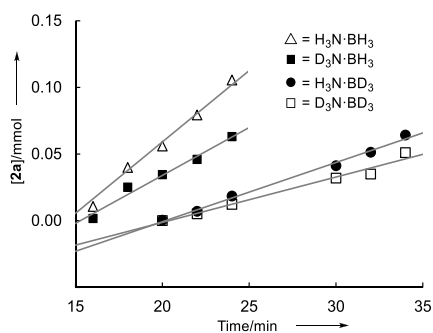
effect of deuterium incorporation in BH$_3$, and KIE$_2$ addresses the impact of deuterium incorporation in NH$_3$. The value of the overall KIE suggests that both B–H and N–H bond-breaking contribute to the rate-determining step, and that is likely if the outer-sphere mechanism is operative. Indeed, multiple previous AB dehydrogenation studies have proved the validity of the outer-sphere mechanism by carefully labeling the substrate and showing that both B–H and N–H bond-breaking influence the total rate.[23] Such a competitive scenario between both inner-sphere and outer-sphere mechanisms have also been observed previously for a bifunctional iridium catalyst, comprising a N-heterocyclic carbene ligand with a tethered alcohol arm.[27]

In the second phase of the reaction, redelivering the stored hydrogen in **I** starts with opening up the thiomethoxy arm to create a vacant site for substrate binding, resulting in intermediate **VI**. This ligand detachment costs a penalty of 11.6 kcal mol^{-1}. The coordination of benzonitrile confers some stability, and bound intermediate **VII** is stabilized by 7.0 kcal mol^{-1} compared to intermediate **VI**. Insertion of a nitrile into the Mn–hydride bond is a relatively facile process and overcomes a barrier of only 19.0 kcal mol^{-1} via **TS-III**. Upon nitrile insertion, reattachment of the thiomethoxy arm leads to intermediate **VIII**, which releases the imine after protonation. Notably, the imine formation marks the completion of the first stage of reduction. The proton migration happens from N–H, and the process is very facile, posing a barrier of only 4.6 kcal mol^{-1} through **TS-IV** (to the energy of intermediate **VIII**). Such a shallow energy barrier for protonation is associated with a low-barrier hydrogen bond,[28] which we have previously observed during alcohol dehydrogenation by **Mn1**.[9] So, the major barrier during the nitrile hydrogenation is the insertion step in manganese hydride, posing a barrier of 19.0 kcal mol^{-1}.

A close look at the alternative pathway of the outer-sphere hydrogenation of the nitrile reveals an asynchronous concerted **TS-VI**, posing a barrier of 17.5 kcal mol^{-1}. This transition state for the hydrogenation maintains a microscopic reversible feature to the outer-sphere transition state for dehydrogenation that follows an asynchronous concerted mechanism.[29] Although the computed energy demand for these outer-sphere and inner-sphere hydrogenation processes are competitive, we feel the nitrile binding via the inner-sphere pathway is important. Additionally, as credible proof of the importance of substrate binding to the metal center, we observe the competence of the thiomethoxy arm to display hemilabile nature as shown in Table 1 (26% yield of **2a** using **Mn4** as a catalyst in comparison to 92% yield using **Mn2**). In fact, the addition of strong Lewis bases, such as pyridine, 4-picoline, and triphenylphosphine, poisons the catalyst easily, drastically reducing the amount of product (18–27% yield of **2a**, Scheme 2), supposedly by blocking the vacant site for nitrile binding to manganese during the inner-sphere hydrogenation process.

Scheme 2. Control Experiments To Prove the Importance of the Hemilabile Arm in the Ligand

Figure 4. Comparison of the initial rates of the **Mn2**-catalyzed formation of **2a** using H$_3$N·H$_3$B and its deuterium isotopologues as the hydrogen source.

Additive	none	PPh$_3$	⬡N	⬡N—CH$_3$
Yield	92%	18%	19%	27%
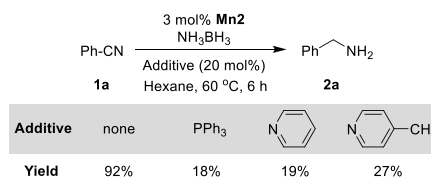
To investigate further in which step the added Lewis base retards the reaction, we conducted a kinetic analysis for the manganese-catalyzed hydrogen evolution from AB in the absence of the nitrile reacting partner (SI, section 7i). As anticipated, the reaction exhibited hydrogen gas evolution. Furthermore, the rate of hydrogen evolution was not hampered significantly when the same reaction was conducted in the presence of an exogenous Lewis base PPh$_3$. A very close rate of hydrogen evolution both in the presence or absence of the phosphine strongly supports our mechanistic hypothesis that the AB dehydrogenation predominantly takes place via an outer-sphere pathway.

This set of control experiments makes us confident about the ligand's participation in the process. Notably, the highest computational barrier of the PES, as calculated, is 20 kcal mol^{-1}. The bulk of this energy demand is in good agreement with the experimentally measured value, $\Delta G_{(298)} = +21.8 \pm 1.5$ kcal mol^{-1} from Eyring analysis (Figure 5). The proximity of
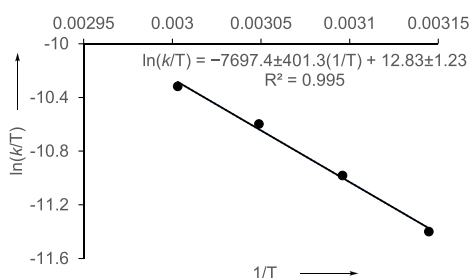
Figure 5. Eyring plot for the **Mn2**-catalyzed transfer hydrogenation of **1a** with AB in THF.

both the experimental and computational barriers is also reassuring regarding the validity of the proposed pathway. Once the imine is formed by the first cycle of reduction, the same process can be repeated via a second cycle to convert the imine into a primary amine, the fully hydrogenated product from benzonitrile.

Furthermore, the synthetic protocol exhibits solvent-dependent chemodivergence in product formation. While a polar protic solvent such as 2-propanol favors secondary amine formation, the aprotic solvent helps the formation of primary amines. In 2-propanol, a primary amine's nucleophilic attack on the imine is likely facilitated by hydrogen bonding offered through a protic solvent. Similarly, the removal of NH$_3$ en route to secondary amines **3** can also be simultaneously helped by solvent-assisted hydrogen bonding. It is intuitive that when such solvent-assisted pathways are not available in aprotic solvents, the second cycle of imine reduction to amine is apparent. Overall, this solvent-dependent tunability offers excellent flexibility in dictating the desired product during the nitrile reduction by AB.

CONCLUSION

In summary, we report the selective conversion of nitriles to primary and secondary amines with bench-stable and phosphine-free homogeneous manganese(I) catalysts using AB as the hydrogen transfer agent under mild reaction conditions. A detailed mechanistic study revealed that the dehydrogenation of AB likely proceeded by an outer-sphere pathway, while the hydrogenation of the nitrile adopted inner-sphere hydrogen transfer. The presence of a hemilabile

thiomethoxy side arm in the catalyst facilitates necessary decoordination to promote inner-sphere substrate hydrogenation. Furthermore, catalyst/solvent-dependent chemodivergence has been discovered, which allows further control in product selectivity. The developed methodology shows excellent functional group tolerance, and the desired amines can be obtained in high yields.

ASSOCIATED CONTENT

Supporting Information

The Supporting Information is available free of charge at https://pubs.acs.org/doi/10.1021/acscatal.0c05406.

> Experimental procedures, analytical data, kinetic data, NMR spectra of compounds and complexes, and computation details (PDF)

AUTHOR INFORMATION

Corresponding Authors

Debashis Adhikari − *Department of Chemical Sciences, Indian Institute of Science Education and Research Mohali, SAS Nagar 140306, India;* orcid.org/0000-0001-8399-2962; Email: adhikari@iisermohali.ac.in

Biplab Maji − *Department of Chemical Sciences, Indian Institute of Science Education and Research Kolkata, Mohanpur 741246, India;* orcid.org/0000-0001-5034-423X; Email: bm@iiserkol.ac.in

Authors

Koushik Sarkar − *Department of Chemical Sciences, Indian Institute of Science Education and Research Kolkata, Mohanpur 741246, India*

Kuhali Das − *Department of Chemical Sciences, Indian Institute of Science Education and Research Kolkata, Mohanpur 741246, India*

Abhishek Kundu − *Department of Chemical Sciences, Indian Institute of Science Education and Research Mohali, SAS Nagar 140306, India*

Complete contact information is available at:
https://pubs.acs.org/10.1021/acscatal.0c05406

Author Contributions

§These authors contributed equally to this work. The manuscript was written through the contributions of all authors. All authors have approved the final version of the manuscript.

Notes

The authors declare no competing financial interest.

REFERENCES

(1) (a) *Non-Noble Metal Catalysis: Molecular Approaches and Reactions*; Wiley, 2019. (b) Chirik, P.; Morris, R. Getting Down to Earth: The Renaissance of Catalysis with Abundant Metals. *Acc. Chem. Res.* **2015**, *48*, 2495−2495.
(2) (a) Anastas, P. T.; Zimmerman, J. B. The periodic table of the elements of green and sustainable chemistry. *Green Chem.* **2019**, *21*,

6545−6566. (b) Bullock, R. M. *Catalysis without Precious Metals*; Wiley-VCH: Weinheim, 2010.

(3) (a) Maji, B.; Barman, M. K. Recent Developments of Manganese Complexes for Catalytic Hydrogenation and Dehydrogenation Reactions. *Synthesis* **2017**, *49*, 3377−3393. (b) Waiba, S.; Maji, B. Manganese Catalyzed Acceptorless Dehydrogenative Coupling Reactions. *ChemCatChem* **2020**, *12*, 1891−1902. (c) Garbe, M.; Junge, K.; Beller, M. Homogeneous Catalysis by Manganese-Based Pincer Complexes. *Eur. J. Org. Chem.* **2017**, *2017*, 4344−4362. (d) Irrgang, T.; Kempe, R. 3d-Metal Catalyzed N- and C-Alkylation Reactions via Borrowing Hydrogen or Hydrogen Autotransfer. *Chem. Rev.* **2019**, *119*, 2524−2549. (e) Filonenko, G. A.; van Putten, R.; Hensen, E. J. M.; Pidko, E. A. Catalytic (de)hydrogenation promoted by non-precious metals - Co, Fe and Mn: recent advances in an emerging field. *Chem. Soc. Rev.* **2018**, *47*, 1459−1483. (f) Valyaev, D. A.; Lavigne, G.; Lugan, N. Manganese organometallic compounds in homogeneous catalysis: Past, present, and prospects. *Coord. Chem. Rev.* **2016**, *308*, 191−235. (g) Hu, Y.; Wang, C. Manganese-Catalyzed C-H Olefination Reactions. *ChemCatChem* **2019**, *11*, 1167−1174. (h) Mukherjee, A.; Milstein, D. Homogeneous Catalysis by Cobalt and Manganese Pincer Complexes. *ACS Catal.* **2018**, *8*, 11435−11469.

(4) Mukherjee, A.; Nerush, A.; Leitus, G.; Shimon, L. J. W.; Ben David, Y.; Espinosa Jalapa, N. A.; Milstein, D. Manganese-Catalyzed Environmentally Benign Dehydrogenative Coupling of Alcohols and Amines to Form Aldimines and H$_2$: A Catalytic and Mechanistic Study. *J. Am. Chem. Soc.* **2016**, *138*, 4298−4301.

(5) Elangovan, S.; Topf, C.; Fischer, S.; Jiao, H.; Spannenberg, A.; Baumann, W.; Ludwig, R.; Junge, K.; Beller, M. Selective Catalytic Hydrogenations of Nitriles, Ketones, and Aldehydes by Well-Defined Manganese Pincer Complexes. *J. Am. Chem. Soc.* **2016**, *138*, 8809−8814.

(6) (a) Pignolet, L. H. *Homogeneous Catalysis with Metal Phosphine Complexes*; Springer, 1983. (b) Zell, T.; Milstein, D. Hydrogenation and Dehydrogenation Iron Pincer Catalysts Capable of Metal−Ligand Cooperation by Aromatization/Dearomatization. *Acc. Chem. Res.* **2015**, *48*, 1979−1994.

(7) (a) Barman, M. K.; Waiba, S.; Maji, B. Manganese-Catalyzed Direct Olefination of Methyl-Substituted Heteroarenes with Primary Alcohols. *Angew. Chem., Int. Ed.* **2018**, *57*, 9126−9130. (b) Jana, A.; Reddy, C. B.; Maji, B. Manganese Catalyzed α-Alkylation of Nitriles with Primary Alcohols. *ACS Catal.* **2018**, *8*, 9226−9231. (c) Barman, M. K.; Jana, A.; Maji, B. Phosphine-Free NNN-Manganese Complex Catalyzed α-Alkylation of Ketones with Primary Alcohols and Friedländer Quinoline Synthesis. *Adv. Synth. Catal.* **2018**, *360*, 3233−3238.

(8) (a) Bruneau-Voisine, A.; Wang, D.; Dorcet, V.; Roisnel, T.; Darcel, C.; Sortais, J.-B. Transfer Hydrogenation of Carbonyl Derivatives Catalyzed by an Inexpensive Phosphine-Free Manganese Precatalyst. *Org. Lett.* **2017**, *19*, 3656−3659. (b) Vasilenko, V.; Blasius, C. K.; Wadepohl, H.; Gade, L. H. Mechanism-Based Enantiodivergence in Manganese Reduction Catalysis: A Chiral Pincer Complex for the Highly Enantioselective Hydroboration of Ketones. *Angew. Chem., Int. Ed.* **2017**, *56*, 8393−8397. (c) van Putten, R.; Benschop, J.; de Munck, V. J.; Weber, M.; Müller, C.; Filonenko, G. A.; Pidko, E. A. Efficient and Practical Transfer Hydrogenation of Ketones Catalyzed by a Simple Bidentate Mn-NHC Complex. *ChemCatChem* **2019**, *11*, 5232−5235. (d) Zhou, Y.-P.; Mo, Z.; Luecke, M.-P.; Driess, M. Stereoselective Transfer Semi-Hydrogenation of Alkynes to E-Olefins with N-Heterocyclic Silylene-Manganese Catalysts. *Chem. - Eur. J.* **2018**, *24*, 4780−4784. (e) Huang, M.; Li, Y.; Li, Y.; Liu, J.; Shu, S.; Liu, Y.; Ke, Z. Room temperature N-heterocyclic carbene manganese catalyzed selective N-alkylation of anilines with alcohols. *Chem. Commun.* **2019**, *55*, 6213−6216. (f) Liu, T.; Wang, L.; Wu, K.; Yu, Z. Manganese-Catalyzed β-Alkylation of Secondary Alcohols with Primary Alcohols under Phosphine-Free Conditions. *ACS Catal.* **2018**, *8*, 7201−7207. (g) Das, K.; Mondal, A.; Srimani, D. Phosphine free Mn-complex catalysed dehydrogenative C-C and C-heteroatom bond formation: a

sustainable approach to synthesize quinoxaline, pyrazine, benzothiazole and quinoline derivatives. *Chem. Commun.* **2018**, *54*, 10582−10585. (h) Papa, V.; Cao, Y.; Spannenberg, A.; Junge, K.; Beller, M. Development of a practical non-noble metal catalyst for hydrogenation of N-heteroarenes. *Nat. Catal.* **2020**, *3*, 135−142.

(9) Jana, A.; Das, K.; Kundu, A.; Thorve, P. R.; Adhikari, D.; Maji, B. A Phosphine-Free Manganese Catalyst Enables Stereoselective Synthesis of (1 + *n*)-Membered Cycloalkanes from Methyl Ketones and 1, *n*-Diols. *ACS Catal.* **2020**, *10*, 2615−2626.

(10) Waiba, S.; Jana, S. K.; Jati, A.; Jana, A.; Maji, B. Manganese complex-catalysed α-alkylation of ketones with secondary alcohols enables the synthesis of β-branched carbonyl compounds. *Chem. Commun.* **2020**, *56*, 8376−8379.

(11) Das, K.; Kumar, A.; Jana, A.; Maji, B. Synthesis and characterization of N,N-chelate manganese complexes and applications in CN coupling reactions. *Inorg. Chim. Acta* **2020**, *502*, 119358.

(12) (a) Garduño, J. A.; García, J. J. Toward Amines, Imines, and Imidazoles: A Viewpoint on the 3d Transition-Metal-Catalyzed Homogeneous Hydrogenation of Nitriles. *ACS Catal.* **2020**, *10*, 8012−8022. (b) Sharma, D. M.; Punji, B. 3d Transition Metal-Catalyzed Hydrogenation of Nitriles and Alkynes. *Chem. - Asian J.* **2020**, *15*, 690−708. (c) Lévay, K.; Hegedüs, L. Recent Achievements in the Hydrogenation of Nitriles Catalyzed by Transitional Metals. *Curr. Org. Chem.* **2019**, *23*, 1881−1900. (d) Bagal, D. B.; Bhanage, B. M. Recent Advances in Transition Metal-Catalyzed Hydrogenation of Nitriles. *Adv. Synth. Catal.* **2015**, *357*, 883−900.

(13) (a) Enthaler, S.; Junge, K.; Addis, D.; Erre, G.; Beller, M. A Practical and Benign Synthesis of Primary Amines through Ruthenium-Catalyzed Reduction of Nitriles. *ChemSusChem* **2008**, *1*, 1006−1010. (b) Reguillo, R.; Grellier, M.; Vautravers, N.; Vendier, L.; Sabo-Etienne, S. Ruthenium-Catalyzed Hydrogenation of Nitriles: Insights into the Mechanism. *J. Am. Chem. Soc.* **2010**, *132*, 7854−7855. (c) Chakraborty, S.; Berke, H. Homogeneous Hydrogenation of Nitriles Catalyzed by Molybdenum and Tungsten Amides. *ACS Catal.* **2014**, *4*, 2191−2194. (d) Choi, J.-H.; Prechtl, M. H. G. Tuneable Hydrogenation of Nitriles into Imines or Amines with a Ruthenium Pincer Complex under Mild Conditions. *ChemCatChem* **2015**, *7*, 1023−1028. (e) Adam, R.; Bheeter, C. B.; Jackstell, R.; Beller, M. A Mild and Base-Free Protocol for the Ruthenium-Catalyzed Hydrogenation of Aliphatic and Aromatic Nitriles with Tridentate Phosphine Ligands. *ChemCatChem* **2016**, *8*, 1329−1334. (f) Saha, S.; Kaur, M.; Singh, K.; Bera, J. K. Selective hydrogenation of nitriles to secondary amines catalyzed by a pyridyl-functionalized and alkenyl-tethered NHC-Ru(II) complex. *J. Organomet. Chem.* **2016**, *812*, 87−94. (g) Konrath, R.; Heutz, F. J. L.; Steinfeldt, N.; Rockstroh, N.; Kamer, P. C. J. Facile synthesis of supported Ru-Triphos catalysts for continuous flow application in selective nitrile reduction. *Chem. Sci.* **2019**, *10*, 8195−8201. (h) Leischner, T.; Spannenberg, A.; Junge, K.; Beller, M. Synthesis of Molybdenum Pincer Complexes and Their Application in the Catalytic Hydrogenation of Nitriles. *ChemCatChem* **2020**, *12*, 4543−4549.

(14) (a) Chen, F.; Topf, C.; Radnik, J.; Kreyenschulte, C.; Lund, H.; Schneider, M.; Surkus, A.-E.; He, L.; Junge, K.; Beller, M. Stable and Inert Cobalt Catalysts for Highly Selective and Practical Hydrogenation of C-N and C-O Bonds. *J. Am. Chem. Soc.* **2016**, *138*, 8781−8788. (b) Elangovan, S.; Topf, C.; Fischer, S.; Jiao, H.; Spannenberg, A.; Baumann, W.; Ludwig, R.; Junge, K.; Beller, M. Selective Catalytic Hydrogenations of Nitriles, Ketones, and Aldehydes by Well-Defined Manganese Pincer Complexes. *J. Am. Chem. Soc.* **2016**, *138*, 8809−8814.

(15) (a) Mukherjee, A.; Srimani, D.; Chakraborty, S.; Ben-David, Y.; Milstein, D. Selective Hydrogenation of Nitriles to Primary Amines Catalyzed by a Cobalt Pincer Complex. *J. Am. Chem. Soc.* **2015**, *137*, 8888−8891. (b) Chakraborty, S.; Milstein, D. Selective Hydrogenation of Nitriles to Secondary Imines Catalyzed by an Iron Pincer Complex. *ACS Catal.* **2017**, *7*, 3968−3972.

(16) Tokmic, K.; Jackson, B. J.; Salazar, A.; Woods, T. J.; Fout, A. R. Cobalt-Catalyzed and Lewis Acid-Assisted Nitrile Hydrogenation to

Primary Amines: A Combined Effort. *J. Am. Chem. Soc.* **2017**, *139*, 13554−13561.

(17) Dai, H.; Guan, H. Switching the Selectivity of Cobalt-Catalyzed Hydrogenation of Nitriles. *ACS Catal.* **2018**, *8*, 9125−9130.

(18) (a) Weber, S.; Stöger, B.; Kirchner, K. Hydrogenation of Nitriles and Ketones Catalyzed by an Air-Stable Bisphosphine Mn(I) Complex. *Org. Lett.* **2018**, *20*, 7212−7215. (b) Weber, S.; Veiros, L. F.; Kirchner, K. Old Concepts, New Application - Additive-Free Hydrogenation of Nitriles Catalyzed by an Air Stable Alkyl Mn(I) Complex. *Adv. Synth. Catal.* **2019**, *361*, 5412−5420.

(19) Garduño, J. A.; García, J. J. Non-Pincer Mn(I) Organometallics for the Selective Catalytic Hydrogenation of Nitriles to Primary Amines. *ACS Catal.* **2019**, *9*, 392−401.

(20) Li, H.; Al-Dakhil, A.; Lupp, D.; Gholap, S. S.; Lai, Z.; Liang, L.-C.; Huang, K.-W. Cobalt-Catalyzed Selective Hydrogenation of Nitriles to Secondary Imines. *Org. Lett.* **2018**, *20*, 6430−6435.

(21) (a) Mai, V. H.; Nikonov, G. I. Transfer Hydrogenation of Nitriles, Olefins, and N-Heterocycles Catalyzed by an N-Heterocyclic Carbene-Supported Half-Sandwich Complex of Ruthenium. *Organometallics* **2016**, *35*, 943−949. (b) Alshakova, I. D.; Gabidullin, B.; Nikonov, G. I. Ru-Catalyzed Transfer Hydrogenation of Nitriles, Aromatics, Olefins, Alkynes and Esters. *ChemCatChem* **2018**, *10*, 4860−4869. (c) Shao, Z.; Fu, S.; Wei, M.; Zhou, S.; Liu, Q. Mild and Selective Cobalt-Catalyzed Chemodivergent Transfer Hydrogenation of Nitriles. *Angew. Chem., Int. Ed.* **2016**, *55*, 14653−14657. (d) Hou, S.-F.; Chen, J.-Y.; Xue, M.; Jia, M.; Zhai, X.; Liao, R.-Z.; Tung, C.-H.; Wang, W. Cooperative Molybdenum-Thiolate Reactivity for Transfer Hydrogenation of Nitriles. *ACS Catal.* **2020**, *10*, 380−390. (e) Sharma, D. M.; Punji, B. Selective Synthesis of Secondary Amines from Nitriles by a User-Friendly Cobalt Catalyst. *Adv. Synth. Catal.* **2019**, *361*, 3930−3936. (f) Garduño, J. A.; Flores-Alamo, M.; García, J. J. Manganese-Catalyzed Transfer Hydrogenation of Nitriles with 2-Butanol as the Hydrogen Source. *ChemCatChem* **2019**, *11*, 5330−5338. (g) Göksu, H.; Ho, S. F.; Metin, Ö.; Korkmaz, K.; Mendoza Garcia, A.; Gültekin, M. S.; Sun, S. Tandem Dehydrogenation of Ammonia Borane and Hydrogenation of Nitro/Nitrile Compounds Catalyzed by Graphene-Supported NiPd Alloy Nanoparticles. *ACS Catal.* **2014**, *4*, 1777−1782. (h) Liu, L.; Liu, Y.; Ai, Y.; Li, J.; Zhou, J.; Fan, Z.; Bao, H.; Jiang, R.; Hu, Z.; Wang, J.; Jing, K.; Wang, Y.; Liang, Q.; Sun, H. Pd-CuFe Catalyst for Transfer Hydrogenation of Nitriles: Controllable Selectivity to Primary Amines and Secondary Amines. *iScience* **2018**, *8*, 61−73.

(22) (a) Staubitz, A.; Robertson, A. P. M.; Manners, I. Ammonia-Borane and Related Compounds as Dihydrogen Sources. *Chem. Rev.* **2010**, *110*, 4079−4124. (b) Zhang, X.; Kam, L.; Trerise, R.; Williams, T. J. Ruthenium-Catalyzed Ammonia Borane Dehydrogenation: Mechanism and Utility. *Acc. Chem. Res.* **2017**, *50*, 86−95. (c) Boom, D. H. A.; Jupp, A. R.; Slootweg, J. C. Dehydrogenation of Amine-Boranes Using p-Block Compounds. *Chem. - Eur. J.* **2019**, *25*, 9133−9152.

(23) Bhattacharya, P.; Krause, J. A.; Guan, H. Mechanistic Studies of Ammonia Borane Dehydrogenation Catalyzed by Iron Pincer Complexes. *J. Am. Chem. Soc.* **2014**, *136*, 11153−11161.

(24) (a) Boyd, T. M.; Andrea, K. A.; Baston, K.; Johnson, A.; Ryan, D. E.; Weller, A. S. A simple cobalt-based catalyst system for the controlled dehydropolymerisation of $H_3B \cdot NMeH_2$ on the gram-scale. *Chem. Commun.* **2020**, *56*, 482−485. (b) Spearing-Ewyn, E. A. K.; Beattie, N. A.; Colebatch, A. L.; Martinez-Martinez, A. J.; Docker, A.; Boyd, T. M.; Baillie, G.; Reed, R.; Macgregor, S. A.; Weller, A. S. The role of neutral Rh(PONOP)H, free NMe_2H, boronium and ammonium salts in the dehydrocoupling of dimethylamine-borane using the cationic pincer $[Rh(PONOP)(\eta^2\text{-}H_2)]^+$ catalyst. *Dalton Trans.* **2019**, *48*, 14724−14736.

(25) Glüer, A.; Förster, M.; Celinski, V. R.; Schmedt auf der Günne, J.; Holthausen, M. C.; Schneider, S. Highly Active Iron Catalyst for Ammonia Borane Dehydrocoupling at Room Temperature. *ACS Catal.* **2015**, *5*, 7214−7217.

(26) (a) Ning, J.; Shang, Z.; Xu, X. How Does the Hemilabile Group in Ruthenium-Cp* Picolyl-NHC Complexes Affect the Mechanism of

Transfer Hydrogenation Reaction? A DFT Study. *Catal. Lett.* **2015**, *145*, 1331−1343. (b) Koga, N.; et al. Role of Agostic Interaction in,&Elimination of Pd and Ni Complexes. An ab Initio MO Study. *J. Am. Chem. Soc.* **1985**, *107*, 7109−7116.

(27) Bartoszewicz, A.; González Miera, G.; Marcos, R. o.; Norrby, P.-O.; Martín-Matute, B. Mechanistic Studies on the Alkylation of Amines with Alcohols Catalyzed by a Bifunctional Iridium Complex. *ACS Catal.* **2015**, *5*, 3704−3716.

(28) Chen, Y.; Liu, S.; Lei, M. Nature of Asynchronous Hydrogen Transfer in Ketone Hydrogenation Catalyzed by Ru Complex. *J. Phys. Chem. C* **2008**, *112*, 13524−13527.

(29) Dub, P. A.; Gordon, J. C. Metal-Ligand Bifunctional Catalysis: The "Accepted" Mechanism, the Issue of Concertedness, and the Function of the Ligand in Catalytic Cycles Involving Hydrogen Atoms. *ACS Catal.* **2017**, *7*, 6635−6655.

■ NOTE ADDED AFTER ASAP PUBLICATION

This paper was published on February 15, 2021. Due to production error, equations 1 and 2 were incorrect. The corrected version was reposted on February 16, 2021.